HHS Public Access

Author manuscript

J Cyst Fibros. Author manuscript; available in PMC 2022 May 07.

Published in final edited form as:

J Cyst Fibros. 2021 January ; 20(1): 165–172. doi:10.1016/j.jcf.2020.09.013.

Airway epithelial stem cell chimerism in cystic fibrosis lung transplant recipients

Don Hayes Jr.[a,c,d,e,h], **Rachael E. Rayner**[g], **Cynthia L. Hill**[b], **Alfahdah Alsudayri**[b], **Mahelet Tadesse**[b], **Scott W. Lallier**[b], **Hemant Parekh**[i], **Guy N. Brock**[f,j], **Estelle Cormet-Boyaka**[g], **Susan D. Reynolds**[b,c,*]

[a]Section of Pulmonary Medicine, Nationwide Children's Hospital, Columbus, OH, USA

[b]Center for Perinatal Research, Nationwide Children's Hospital, Columbus, OH, USA

[c]Departments of Pediatrics, The Ohio State University College of Medicine, Columbus, OH, USA

[d]Internal Medicine, The Ohio State University College of Medicine, Columbus, OH, USA

[e]Surgery, The Ohio State University College of Medicine, Columbus, OH, USA

[f]Biomedical Informatics, The Ohio State University College of Medicine, Columbus, OH, USA

[g]Department of Veterinary Biosciences, The Ohio State University College of Veterinary Medicine, Columbus, OH, USA

[h]Division of Pulmonary, Critical Care, and Sleep Medicine, The Ohio State University Wexner Medical Center, Columbus, OH, USA

[i]Clinical Histocompatibility/Tissue Typing Laboratory, The Ohio State University Wexner Medical Center, Columbus, OH, USA

[j]Center for Biostatistics and Bioinformatics, The Ohio State University Wexner Medical Center, Columbus, OH, USA

Abstract

*Corresponding author. susan.reynolds@nationwidechildrens.org (S.D. Reynolds).

Author participation

DH: Conception and design, acquisition of clinical samples and data, interpretation of data, drafting of the manuscript
RR: Acquisition of laboratory data, reviewing of manuscript
CLH: Acquisition of laboratory data, reviewing of manuscript
AA: Acquisition of laboratory data, reviewing of manuscript
MT: Acquisition of laboratory data, reviewing of manuscript
SWL: Acquisition of laboratory data, reviewing of manuscript
HP: Acquisition of laboratory data, interpretation of data, reviewing of manuscript
GNB: Statistical analysis, interpretation of data, reviewing of manuscript
ECB: Acquisition of laboratory data, interpretation of data, reviewing of manuscript
SDR: Conception and design, acquisition of laboratory data, interpretation of data, manuscript preparation.

Ethics statement

The Institutional Review Board at Nationwide Children's Hospital approved the study. Written informed consent and assent was obtained from every participant.

Declaration of Competing Interest

The authors report no conflicts of interest and have no relevant disclosures.

Supplementary materials

Supplementary material associated with this article can be found, in the online version, at doi:10.1016/j.jcf.2020.09.013.

Background: The conducting airway epithelium is repaired by tissue specific stem cells (TSC). In response to mild/moderate injury, each TSC repairs a discrete area of the epithelium. In contrast, severe epithelial injury stimulates TSC migration and expands the stem cell's reparative domain. Lung transplantation (LTx) can cause a moderate/severe airway injury and the remodeled airway contains a chimeric mixture of donor and recipient cells. These studies supported the hypothesis, LTx stimulates TSC migration resulting in epithelial chimerism. We tested this hypothesis in cystic fibrosis (CF) LTx patients.

Methods: Airway mucosal injury was quantified using bronchoscopic imaging and a novel grading system. Bronchial brushing was used to recover TSC from 10 sites in the recipient and allograft airways. TSC chimerism was quantified by short tandem repeat analysis. TSC self-renewal and differentiation potential were assayed using the clone forming cell frequency and air-liquid-interface methods. Electrophysiology was used to determine if TSC chimerism altered epithelial ion channel activity.

Results: LTx caused a mild to moderate airway mucosal injury. Donor and recipient TSC were identified in 91% of anastomotic sites and 93% of bronchial airways. TSC chimerism did not alter stem cell self-renewal or differentiation potential. The frequency of recipient TSC was proportional to CF Transmembrane Conductance Regulator (CFTR)-dependent ion channel activity and 33% of allograft regions were at risk for abnormal CFTR activity.

Conclusions: LTx in CF patients stimulates bidirectional TSC migration across the anastomoses. TSC chimerism may alter ion homeostasis and compromise the host defense capability of the allograft airway epithelium.

Keywords

Airway epithelial stem cell; Chronic lung allograft dysfunction; Cystic fibrosis; Lung transplant; Basal cell

1. Introduction

Cystic fibrosis (CF) is a multisystem disease that is caused by mutations in the CF Transmembrane Conductance Regulator (CFTR) gene [1]. Although clinical advancements have significantly extended the life expectancy of people with CF, respiratory failure remains the major cause of death. Consequently, CF is the most frequent indication for lung transplant (LTx) in children and is the third most common indication for LTx in adults [2]. Although survival of CF patients is the longest among all LTx patients, most CF LTx patients develop chronic lung allograft dysfunction (CLAD).

Many LTx patients develop obstructive allograft dysfunction, a lesion that is limited to small airway segments [3]. However, numerous studies in human patients (reviewed in [4]) and animal models [5, 6] indicate that disease is initiated by bronchial epithelial injury. Subsequently, an aberrant repair process decreases the frequency of airway epithelial secretory and ciliated cells and reduces mucociliary function. These epithelial changes may compromise host defense within the allograft (reviewed in [7]).

The remodeled allograft airway contains a mixture of donor and recipient epithelial cells [8–11]. This chimerism develops within days of LTx and persists for years [9]. Medawar proposed that recipient cells protected the allograft from immune-mediated damage (https://doi.org/10.1093/oxfordjournals.bmb.a070392). However, later studies correlated bronchial injury with the frequency of recipient epithelial cells and suggested that these cells were repairing the damaged allograft epithelium [9, 12]. Existing data do not distinguish between the protective and reparative mechanisms.

The human bronchial epithelium is repaired by resident tissue stem cells (TSC, reviewed in [13]). Analysis of TSC in animal models demonstrated that mild to moderate injury activates TSC with a basal and/or Club cell phenotype [14–16]. These TSC proliferate and produce two daughter cells: one cell remains a stem cell while the second cell generates differentiated cell types. In contrast, severe injury promotes TSC migration to the injury site [17–20]. Several studies reported that TSC number decreases after LTx [5, 21, 22] and this decline was correlated with CLAD [5]. The mechanism leading to TSC depletion was not determined.

Reports of moderate to severe allograft injury suggested that epithelial chimerism might result from mixing of the donor and recipient TSC pools. Thus, we hypothesized: LTx stimulates TSC migration resulting in epithelial chimerism. We tested this hypothesis in CF LTx patients. Our aims were to: 1) quantify bronchial epithelial injury; 2) quantify TSC chimerism; and 3) model the effects of chimerism on epithelial structure and function.

2. Methods

Complete methods:

Please see Supplemental Information.

Patient cohort:

This study enrolled 10 consecutive lung transplantation (LTx) patients over one calendar year. No patients were excluded, and all patients gave written consent/assent to participate. LTx recipient and lung donor demographics are presented in Supplemental (S) Table 1. The immunosuppression protocol and treatment for acute cellular rejection are detailed in Supplemental Information.

Surveillance flexible fiberoptic bronchoscopy (sFFB) and mucosal imaging:

All subjects were clinically stable at the time of sFFB and were being evaluated for silent rejection. The LTx literature contains numerous analyses of anastomotic damage [23]. However, mucosal injury distal to the anastomosis has received less attention. To fill this knowledge gap, we used bronchoscopic imaging to evaluate mucosal changes 1 cm distal to the left and right anasto-moses. These sites were evaluated on post-LTx day 14 which co-incided the typical period of LTx-associated mucosal injury and a sFBB. Anastomotic complications, including dehiscence, stenosis, and malacia, were not detected. Initially, allograft regions were imaged, and these data were used to evaluate ischemia, edema, and sloughing. Next, a single gentle tap of the suction channel was performed. In our experience,

this gentle maneuver does not alter a normal healthy airway but reveals inflammation and friability in abnormal airways. The regions were reimaged, and the second image was evaluated for erythema.

Quantification of mucosal injury:

The most recent International Society for Heart and Lung Transplantation scoring system [23] focuses on ischemia, necrosis, dehiscence, stenosis, and malacia. However, this system does not quantify airway mucosal injury. To fill this gap, archived images were scored by three pulmonologists using a novel Airway Mucosal Injury Index (STable 2). Scorers were blinded to the diagnosis. The three scores were averaged. All 10 subjects participated in this study.

Airway mucosa sampling:

Mucosal sampling was conducted during a sFFB and used a protected 1.8 mm bronchial cytology brush (Olympus Corporation, Tokyo, Japan). The 10 pre-determined sampling sites are listed in Fig 2 A and are based on a study by Franklin and colleagues [24]. This sampling pattern was intended to survey the bronchial airways and as such may not represent the entire allograft. Some sites were sampled twice. Consequently, a total of 135 samples were analyzed. All 10 subjects participated in this study. STable 3 presents the interval between LTx and sampling (average 1482 days, range 34–9393 days) and clinical parameters at the time of sampling.

TSC selection:

Mucosal cells were recovered from the brush as previously reported [25], with the exception that 14.3 μM 2-mercaptoethanol was used to remove mucus. Since a prospective TSC purification protocol has not been developed, TSC were selected using the modified conditional reprogramming culture (mCRC) method [26]. Some brushings were used to generate duplicate passage 0 cultures (see below). All passage 1 cells expressed the TSC markers CD49f and Tissue Factor 1 and were negative for CD45 (hematopoietic cells), CD31 (endothelial cells), and CD90 (fibroblasts) (data not shown).

TSC function studies:

For life-span analyses, TSC were sub-cultured and harvested at 80% confluence. TSC self-renewal was quantified at each passage using the clone-forming cell frequency (CFCF) assay [27]. To evaluate differentiation potential, TSC were plated onto Transwell membranes [25]. At confluence, the medium was changed to PneumaCult ALI (Stemcell Technologies, Vancouver, BC, CA). On day 21, differentiation was quantified as previously reported [26].

Chimerism analysis:

The Promega PowerPlex® 16 HS system (STR, Promega Corporation, Madison, WI, USA) was used to determine the relative frequency of recipient and donor genomes in passage 1 TSC. This approach allowed us to evaluate chimerism using a prospective, cross-sectional study design and include same sex donor and recipient pairs. Controls were archived pre-transplantation STR data for donors and recipients and TSC from the recipient's nasal

respiratory epithelium. Analysis of duplicate cultures demonstrated less than 1% variation between the two samples (data not shown). Results are presented as the percent of TSC which were derived from the recipient.

Statistical methods:

Normally distributed data sets were evaluated by Student's *t*-test and data sets that exhibited non-normal distributions were analyzed by the Mann-Whitney test. Data sets containing multiple variables were analyzed by analysis of variance (ANOVA) and a post hoc Tukey test or Kruskal Willis test. Regression analysis was conducted using the linear model. Significance was indicated by $p \leq 0.05$.

3. Results

Airway mucosal injury:

Fig 1A–D uses images from two patients illustrate mucosal injury. In patient 1, large strands of mucosal tissue were found in the left allograft (Fig 1A) and smaller strands of mucosal tissue were found in the right allograft (Fig 1B). In patient 2, the left allograft (Fig 1C) exhibits hyperemic airways, edema leading to blunting of the subsegmental carina, blue-black appearance of the mucosa involving 10–50% of the visualized field and sloughing with small strands of mucosal tissue. The right allograft (Fig 1D) demonstrates moderately red airways with linear submucosal hemorrhage, edema leading to loss of airway architecture, blue-black appearance of the mucosa involving <10% of the visualized field and sloughing with large strands of mucosal tissue.

The Airway Mucosal Injury Index (STable 2) was used to quantify mucosal injury. The Total Injury Score identified mild to severe mucosal injury in the left and right allograft of all subjects (Fig 1E). Ischemia was identified in 90% of subjects and was bilateral in 70% of patients (Fig 1F). Ischemia ranged from mild to severe. This distribution was skewed by significantly greater ischemia scores in the left allograft (data not shown). Erythema, edema, and sloughing were observed in all subjects and ranged from mild to severe (Fig 1F). The Total Injury Score did not predict a CLAD diagnosis (Fig 1G). These data demonstrated that the bronchial mucosa underwent a mild to moderate injury within 14 days of LTx.

TSC self-renewal and life-span:

Our previous analysis demonstrated that TSC self-renewal was similar in non-CF and CF patients [25]. To extend this analysis to LTx, we compared the CFCFx1000 for TSC that were recovered from bronchial airways (Fig 2A). No significant differences were detected across the 10 sampling sites (Fig 2B). Further, the CFCFx1000 values for TSC recovered from LTx subjects were comparable to those observed in CF patients who were undergoing sinus surgery [25], Fig 2B). We did not detect a change in CFCFx1000 as a function of time after LTx (data not shown). These data indicate that LTx does not alter the self-renewal potential of TSC.

Our previous study used the CFCF assay to demonstrate that TSC can be divided into short-lived and long-lived subsets [25]. Short-lived TSC were lost over passages 1–5. Most long-

lived TSC could be maintained through passage 10–20, while a few TSC could be passaged more than 20 times. The CFCFx10 0 0 of long-lived TSC was 150–200. To evaluate the longevity of allograft TSC, 6 samples were serially passaged (Fig 2C). CFCFx1000 was similar at passages 1 and 2 and decreased to ~150 at passage 5. A similar pattern was observed for TSC recovered from the bronchial airways of CF patients [25], Fig 2C). These data indicated that the allograft contained both short-lived and long-lived TSC and that the lifespan of donor TSC was similar to that of TSC recovered from CF patients.

Selection does not alter the representation of non-CF and CF TSC:

Quantification of TSC chimerism requires selection of TSC and amplification to levels that meet the sensitivity threshold for STR analysis. To authenticate this approach, we modeled chimerism using TSC from non-CF and CF donors (Supplemental Information, SFig 1). The non-CF TSC were tagged with eGFP and the CF TSC were tagged with mCherry. Tagged cells were mixed at various ratios and plated (SFig 1A). Because TSC clones contain both TSC and non-TSC [15], the CFCF was determined and used to calculate the number of non-CF and CF TSC that were plated. At 80% confluence, the frequency of eGFP and mCherry tagged cells was determined by flow cytometry. Regression analysis demonstrated that the representation of non-CF and CF TSC did not change during proliferation (SFig 1D). A similar study switched the tags and confirmed these results for proliferation (SFig 1B, E) and differentiation (SFig1C, F). Collectively, these data indicated that selection did not alter the representation of non-CF and CF TSC.

Chimerism within the TSC pool:

Analysis of TSC from the nasal passages indicated that all cells were from the recipient and demonstrated the specificity of the STR assay (Fig 3A). Analysis of the anastomoses demonstrated chimerism within the recipient and allograft broncus (Fig 3B). Of the 56 samples, 51 (91%) exhibited mixing of donor and recipient TSC. The frequency of recipient TSC (%Recipient TSC) was 8–100% in recipient airways and 0–96% in the allograft. The %Recipient TSC was significantly greater in the recipient bronchi. Chimerism at the anastomoses did not correlate with the total or individual injury scores (data not shown).

Analysis of the allograft identified chimerism within each of the 6 sampling sites (Fig 3C). Of the 82 samples, 76 (93%) exhibited mixing of donor and recipient TSC. The extent of this chimerism ranged from 0–98% across the six sampling sites. The %Recipient TSC was significantly greater in the right upper lobe relative to the right lower lobe but did not vary across the other sampling sites. TSC chimerism in the allograft did not correlate with the total or individual injury scores (data not shown). Collectively, these data support the conclusion that LTx promotes bidirectional TSC migration across the anastomosis.

TSC chimerism does not predict a CLAD diagnosis:

One of our original goals was to determine if TSC chimerism could be used as a biomarker for CLAD. A comparison of TSC chimerism and CLAD score (STable 3) demonstrated increased chimerism with a CLAD score of 3 (Fig 3D). However, this correlation was not observed in other comparisons. We then used a mixed model to evaluate differences between subjects who had CLAD at the time of sampling and those who were free of

CLAD (Fig 3E). The response variable was %Recipient TSC. The mean difference was 9.8% and the difference was not significant ($p = 0.48$). If the analysis was limited to the left upper lobe, a significant relationship between %Recipient TSC and CLAD was found (mean difference = 48%, $p = 0.025$). However, a similar analysis of the right upper lobe did not find a relationship between %Recipient TSC and CLAD. These results indicated that TSC chimerism was not predictive of CLAD.

Impact of TSC chimerism on differentiation:

TSC from sampling sites 1–6 were used to generate air-liquid-interface (ALI) cultures that were differentiated in PneumaCult ALI medium. Differentiation to ACT-positive ciliated cells (Fig 4 A, C) or MUC5B-positive goblet cells (Fig 4 B, D) did not vary as a function of TSC chimerism. These data indicated that donor and recipient TSC exhibited multi-lineage differentiation.

Impact of chimerism on airway ion channel function:

Previous studies demonstrated that chloride ion homeostasis was normal in cultures containing 10–50% non-CF cells (reviewed in [1]). In this study, we first modeled chimerism using pure populations of non-CF and CF TSC that were differentiated using Pneumacult ALI medium. Ussing chamber analysis demonstrated that CFTR dependent current was proportional to the frequency of non-CF TSC (Fig 5A).

Analysis of allograft TSC cultures demonstrated that CFTR dependent short-circuit current (Fig 5B) varied with the frequency of donor (non-CF) cells. In contrast, Epithelial Sodium Channel (ENaC) dependent short circuit current (Fig 5C) and transepithelial electrical current (Fig 5D) did not correlated with the frequency of donor cells. These data indicate that TSC chimerism impacts CFTR function.

4. Discussion

Previous studies identified bronchial epithelial chimerism in every allograft that underwent analysis [8, 9, 11, 12]. We now report that this chimerism includes TSC (Fig 3 B–C). We detected TSC chimerism in all subjects, at multiple locations in the allograft, and in the recipient airways. These data indicate that TSC migrate in response to LTx and that this migration is bidirectional.

TSC mediate epithelial repair and studies in animals indicated that severe injury stimulated TSC migration toward the injury site [17–20]. This concept was extended to LTx by a previous chimerism study in which the frequency of recipient epithelial cells was increased in regions with chronic injury [9]. Our study reinforces this association. However, our quantification of mucosal injury (Fig 1) suggests that a mild injury can stimulate TSC migration in LTx patients.

In contrast with lung, epithelial chimerism in liver allografts has been extensively analyzed (reviewed in [28]). Histological methods reported that 1–3% of hepatocytes were recipient derived. In contrast, a report which used laser capture microdissection and STR analysis reported that 55% of hepatocytes were recipient derived and that this chimerism increased

to 67% in subjects with recurrent hepatitis [29]. Variation across these studies suggests that chimerism may be underreported by histological approaches. In the lung allograft, histological studies reported that bronchial epithelial chimerism was 1–6% [8); whereas, chimerism was 6–24% in studies that used the STR method [9, 11]. In our study, the median %Recipient TSC ranged from 8 to 59.5% in allograft bronchi and 6 to 39.5% in allograft bronchial airways. While TSC chimerism has not been previously evaluated in solid organ allografts, the extent of TSC chimerism detected in our study is similar to the level of epithelial chimerism which was quantified using STR.

We previously reported that non-CF and CF TSC had the same mitotic and differentiation potential in vitro [25]. This conclusion was extended to airways by a single cell RNAseq analysis of freshly isolated lung cells (bioRxiv 2020.05.01.072876). This study reported that the number and frequency of conducting airway epithelial cell types did not vary between non-CF and CF. Collectively, these data sets indicate that non-CF and CF TSC have the same proliferation and the same differentiation potential in vivo and in vitro. The present study indicates that proliferation and differentiation of chimeric TSC was comparable to those of TSC recovered from the bronchial airways of living CF donors ((25), Figs. 2 and 4). Our demonstration that CFTR-dependent short circuit current was proportional to the %Recipient TSC (Fig 5B) raises the possibility that the allograft epithelium is a mosaic of non-CF and CF phenotypes. Based on the finding that CF carriers have an increased risk of airway disease [30], our data suggest that ~33% of allograft regions were at risk for a significant decrease in CFTR-dependent ion channel activity and associated alterations in host defense capacity [7].

Our CFCF data suggested that LTx does not alter TSC number (Fig 2 B, C). However, a study by Swatek and colleagues reported that LTx depleted the TSC population in ferrets [5]. The cause of this discrepancy is not known. Swatek and colleagues also reported that the extent of TSC depletion correlated with allograft rejection grade. In contrast with these results, we did not find an association between injury on post-LTx day 14 and CLAD (Fig 1 G), %Recipient TSC and CLAD score (Fig 3D), or %Recipient TSC and initiation of CLAD (Fig 3E). Our inability to associate our results with CLAD may be due to limitations in our study design including a single-center analysis of a small and heterogeneous patient cohort with progressing rather than end-stage CLAD (STable 3). In addition, severe injury was previously associated with activation of reserve myoepithelial stem cells [17–19]. While we cannot exclude the possibility that these cells were included in our TSC preparations [17,18), this possibility is diminished by reports that LTx results in destruction of submucosal glands in human patients and in ferrets [5] and the limited life-span of myoepithelial stem cells in vitro [17]. Future studies are needed to overcome the limitations of our study and to resolve differences between our results and those of our colleagues.

5. Conclusion

This study establishes TSC chimerism as a fundamental component of allograft pathology and suggests that TSC chimerism may compromise host defense in the allograft of CF LTx patients.

Supplementary Material

Refer to Web version on PubMed Central for supplementary material.

Acknowledgements

This project was funded by Research grants from the Cystic Fibrosis Foundation (REYNOL17XXO, REYNOL19XXO, Nationwide Children's Hospital Cellular Therapy and Cancer Immunotherapy Program, Cystic Fibrosis Foundation Cure Columbus Research Development Program and the Epithelial Cell Core (C3RDP, MCCOY19R0). Cynthia M. Schwartz, MD generated the graphic in Fig 2A. The authors thank Benjamin T. Kopp for his constructive comments.

References

[1]. Elborn JS. Cystic fibrosis. Lancet 2016.

[2]. Hayes D Jr, Cherikh WS, Chambers DC, Harhay MO, Khush KK, Lehman RR, et al. The International Thoracic Organ Transplant Registry of the International Society for Heart and Lung Transplantation: twenty-second pediatric lung and heart-lung transplantation report-2019; Focus theme: donor and recipient size match. J Heart Lung Transplant 2019;38(10):1015–27. [PubMed: 31548028]

[3]. Verleden SE, Vasilescu DM, Willems S, Ruttens D, Vos R, Vandermeulen E, et al. The site and nature of airway obstruction after lung transplantation. Am J Respir Crit Care Med 2014;189(3):292–300. [PubMed: 24354907]

[4]. Fernandez IE, Heinzelmann K, Verleden S, Eickelberg O. Characteristic patterns in the fibrotic lung. Comparing idiopathic pulmonary fibrosis with chronic lung allograft dysfunction. Ann Am Thorac Soc 2015;12(1):S34–41 Suppl. [PubMed: 25830833]

[5]. Swatek AM, Lynch TJ, Crooke AK, Anderson PJ, Tyler SR, Brooks L, et al. Depletion of airway submucosal glands and TP63(+)KRT5(+) basal cells in obliterative bronchiolitis. Am J Respir Crit Care Med 2018;197(8):1045–57. [PubMed: 29236513]

[6]. Qu N, de Vos P, Schelfhorst M, de Haan A, Timens W, Prop J. Integrity of airway epithelium is essential against obliterative airway disease in transplanted rat tracheas. J Heart Lung Transplant 2005;24(7):882–90. [PubMed: 15982618]

[7]. Sato M, Keshavjee S. Bronchiolitis obliterans syndrome: alloimmune-dependent and -independent injury with aberrant tissue remodeling. Semin Thorac Cardiovasc Surg 2008;20(2):173–82. [PubMed: 18707652]

[8]. Spencer H, Rampling D, Aurora P, Bonnet D, Hart SL, Jaffe A. Transbronchial biopsies provide longitudinal evidence for epithelial chimerism in children following sex mismatched lung transplantation. Thorax 2005;60(1):60–2. [PubMed: 15618585]

[9]. Kleeberger W, Versmold A, Rothamel T, Glockner S, Bredt M, Haverich A, et al. Increased chimerism of bronchial and alveolar epithelium in human lung allografts undergoing chronic injury. Am J Pathol 2003;162(5):1487–94. [PubMed: 12707031]

[10]. Murakawa T, Kerklo MM, Zamora MR, Wei Y, Gill RG, Henson PM, et al. Simultaneous LFA-1 and CD40 ligand antagonism prevents airway remodeling in orthotopic airway transplantation: implications for the role of respiratory epithelium as a modulator of fibrosis. J Immunol 2005;174(7):3869–79. [PubMed: 15778341]

[11]. May LA, Kicic A, Rigby P, Heel K, Pullen TL, Crook M, et al. Cells of epithelial lineage are present in blood, engraft the bronchial epithelium, and are increased in human lung transplantation. J Heart Lung Transplant 2009;28(6):550–7. [PubMed: 19481014]

[12]. Paivaniemi OE, Musilova P, Raivio PM, Maasilta PK, Alho HS, Rubes J, et al. Ingraft chimerism in lung transplantation–a study in a porcine model of obliterative bronchiolitis. Respir Res 2011;12:56. [PubMed: 21521503]

[13]. Liu X, Engelhardt JF. The glandular stem/progenitor cell niche in airway development and repair. Proc Am Thorac Soc 2008;5(6):682–8. [PubMed: 18684717]

[14]. Hong KU, Reynolds SD, Watkins S, Fuchs E, Stripp BR. Basal cells are a multipotent progenitor capable of renewing the bronchial epithelium. Am J Pathol 2004;164(2):577–88. [PubMed: 14742263]

[15]. Ghosh M, Smith RW, Runkle CM, Hicks DA, Helm KM, Reynolds SD. Regulation of trachebronchial tissue-specific stem cell pool size. Stem Cells 2013;31(12):2767–78. [PubMed: 23712882]

[16]. Rock JR, Onaitis MW, Rawlins EL, Lu Y, Clark CP, Xue Y, et al. Basal cells as stem cells of the mouse trachea and human airway epithelium. PNAS 2009;106(31):12771–5. [PubMed: 19625615]

[17]. Lynch TJ, Anderson PJ, Rotti PG, Tyler SR, Crooke AK, Choi SH, et al. Submucosal gland myoepithelial cells are reserve stem cells that can regenerate mouse tracheal epithelium. Cell Stem Cell 2018;22(5):653–67 e5. [PubMed: 29656941]

[18]. Tata A, Kobayashi Y, Chow RD, Tran J, Desai A, Massri AJ, et al. Myoepithelial cells of submucosal glands can function as reserve stem cells to regenerate airways after injury. Cell Stem Cell 2018;22(5):668–83 e6. [PubMed: 29656943]

[19]. Kumar PA, Hu Y, Yamamoto Y, Hoe NB, Wei TS, Mu D, et al. Distal airway stem cells yield alveoli in vitro and during lung regeneration following H1N1 influenza infection. Cell 2011;147(3):525–38. [PubMed: 22036562]

[20]. Vaughan AE, Brumwell AN, Xi Y, Gotts JE, Brownfield DG, Treutlein B, et al. Lineage-negative progenitors mobilize to regenerate lung epithelium after major injury. Nature 2015;517(7536):621–5. [PubMed: 25533958]

[21]. Kelly FL, Kennedy VE, Jain R, Sindhwani NS, Finlen Copeland CA, Snyder LD, et al. Epithelial clara cell injury occurs in bronchiolitis obliterans syndrome after human lung transplantation. Am J Transplant 2012;12(11):3076–84. [PubMed: 22883104]

[22]. Gilpin SE, Lung KC, Sato M, Singer LG, Keshavjee S, Waddell TK. Altered progenitor cell and cytokine profiles in bronchiolitis obliterans syndrome. J Heart Lung Transplant 2012;31(2):222–8. [PubMed: 22305385]

[23]. Crespo MM, McCarthy DP, Hopkins PM, Clark SC, Budev M, Bermudez CA, et al. ISHLT consensus statement on adult and pediatric airway complications after lung transplantation: definitions, grading system, and therapeutics. J Heart Lung Transplant 2018;37(5):548–63. [PubMed: 29550149]

[24]. Franklin WA, Gazdar AF, Haney J, Wistuba II, La Rosa FG, Kennedy T, et al. Widely dispersed p53 mutation in respiratory epithelium. A novel mechanism for field carcinogenesis. J Clin Investig 1997;100(8):2133–7. [PubMed: 9329980]

[25]. Hayes D Jr, Kopp BT, Hill CL, Lallier SW, Schwartz CM, Tadesse M, et al. Cell therapy for cystic fibrosis lung disease: regenerative basal cell amplification. Stem Cells Transl Med 2018.

[26]. Reynolds SD, Rios C, Wesolowska-Andersen A, Zhuang Y, Pinter M, Happoldt C, et al. Airway progenitor clone formation is enhanced by Y-27632-dependent changes in the transcriptome. Am J Respir Cell Mol Biol 2016.

[27]. Ghosh M, Helm KM, Smith RW, Giordanengo MS, Li B, Shen H, et al. A single cell functions as a tissue-specific stem cell and the in vitro niche-forming cell. Am J Respir Cell Mol Biol 2011;45(3):459–69. [PubMed: 21131442]

[28]. Lehmann U, Versmold A, Kreipe H. Combined laser-assisted microdissection and short tandem repeat analysis for detection of in situ microchimerism after solid organ transplantation. Methods Mol Biol 2005;293:113–23. [PubMed: 16028415]

[29]. Kleeberger W, Rothamel T, Glockner S, Flemming P, Lehmann U, Kreipe H. High frequency of epithelial chimerism in liver transplants demonstrated by microdissection and STR-analysis. Hepatology 2002;35(1):110–16. [PubMed: 11786966]

[30]. Miller AC, Comellas AP, Hornick DB, Stoltz DA, Cavanaugh JE, Gerke AK, et al. Cystic fibrosis carriers are at increased risk for a wide range of cystic fibrosis-related conditions. PNAS 2019.

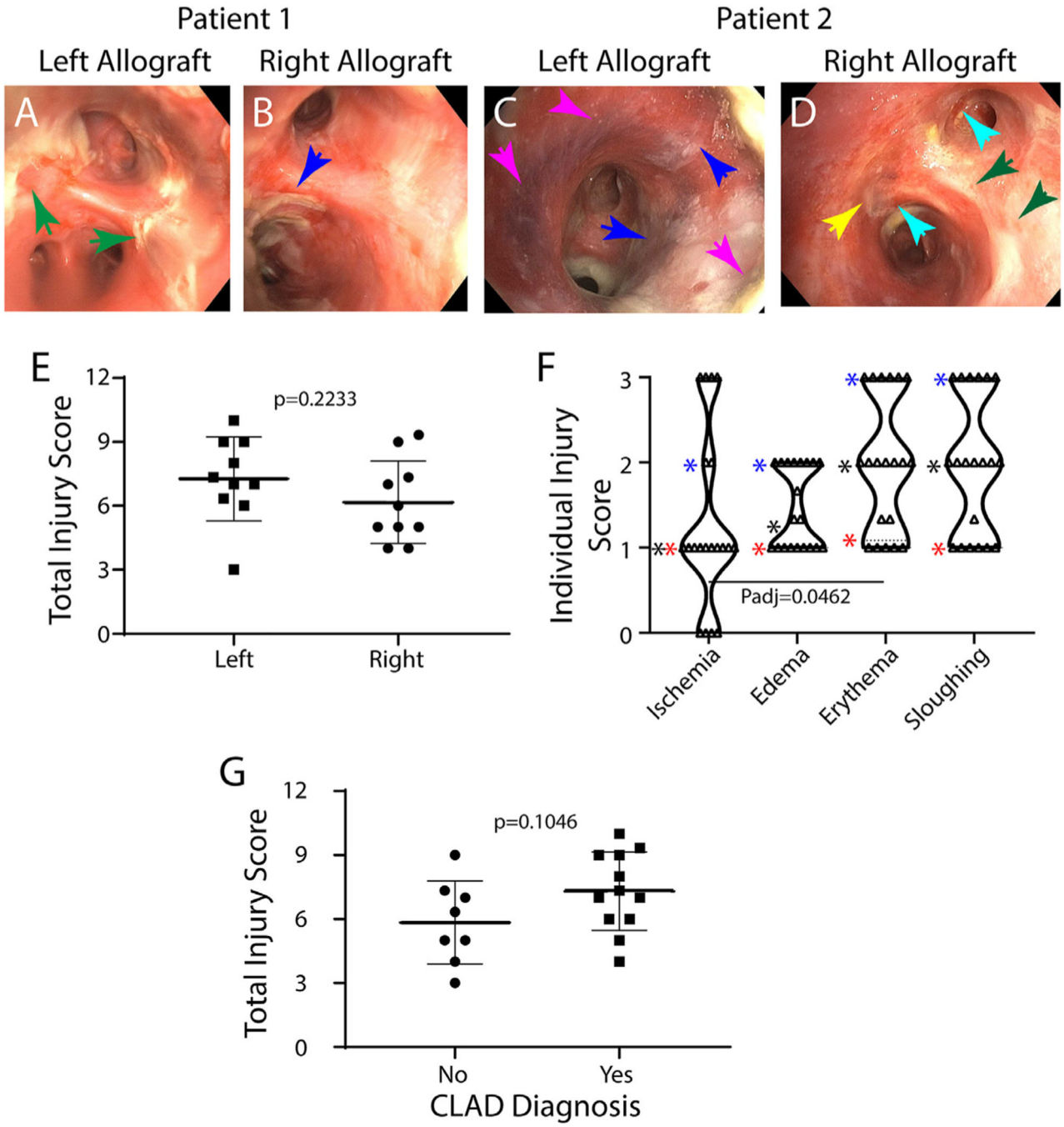

Fig 1.

Airway mucosal injury. A–D: Bronchoscopy images representing airway mucosal changes that occur 14 days after lung transplantation. Images of the left (A, C) and right (B, D) bronchus 1 cm distal to the anastomosis are presented for Patients 1 (A, B) and 2 (C, D). Arrows: green; sloughing score of 3; blue, sloughing score of 2; pink, ischemia score of 2; yellow, ischemia score of 1; turquoise, erythema score of 2. E: Total injury scores for the left and right allograft were determined as described in STable 2. Symbols represent values for each patient. Data are presented as the mean ± standard deviation. Differences were

evaluated by Student's *t*-test. F. Individual injury scores. Symbols represent values for the left and right allograft for each patient. Data are presented as violin plots. Stars: blue-75th percentile, black-median, red-25th percentile. Differences were evaluated by Kruskal-Wallis test. G. Total injury score as a function of CLAD diagnosis. Data are presented as the mean ± standard deviation. Differences were evaluated by Student's *t*-test. (For interpretation of the references to color in this figure legend, the reader is referred to the web version of this article.)

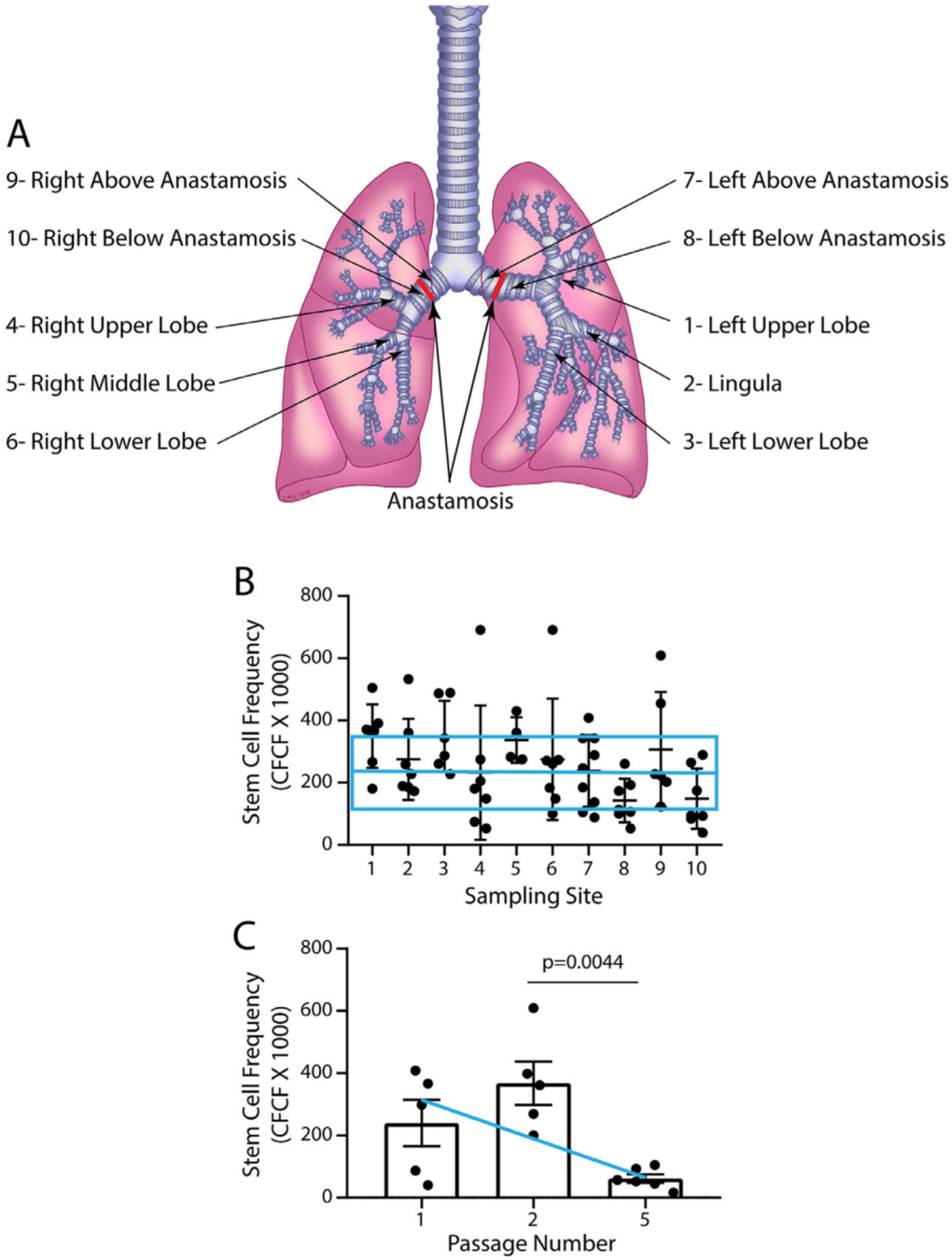

Fig 2.

TSC frequency and longevity. A. Sampling locations. 1, left upper lobe; 2, lingula; 3, left lower lobe; 4, right upper lobe; 5, right middle lobe; 6, right lower lobe; 7, left bronchus above the anastomosis; 8, left bronchus below the anastomosis; 9, right bronchus above the anastomosis; 10, right bronchus below the anastomosis. B. The clone forming cell frequency (CFCF) assay was used to determine the frequency of TSC at various sampling sites. The horizontal blue line and box represent the average CFCFx10 0 0 and standard deviation for CF patients who were sampled during sinus surgery [25]. Symbols represent individual data

points. Data are presented as the medial and interquartile range, $n = 6–10$. Differences were evaluated by Kruskal-Wallis test. C. CFCFx10 0 0 was examined in a subset of samples that were serially passaged. The blue line indicates the average CFCFx10 0 0 for CF patients who were sampled during sinus surgery [25]. Symbols represent individual data points. Data are presented as the mean ± standard deviation, $n = 5–6$. Differences were evaluated by Student's *t*-test. (For interpretation of the references to color in this figure legend, the reader is referred to the web version of this article.)

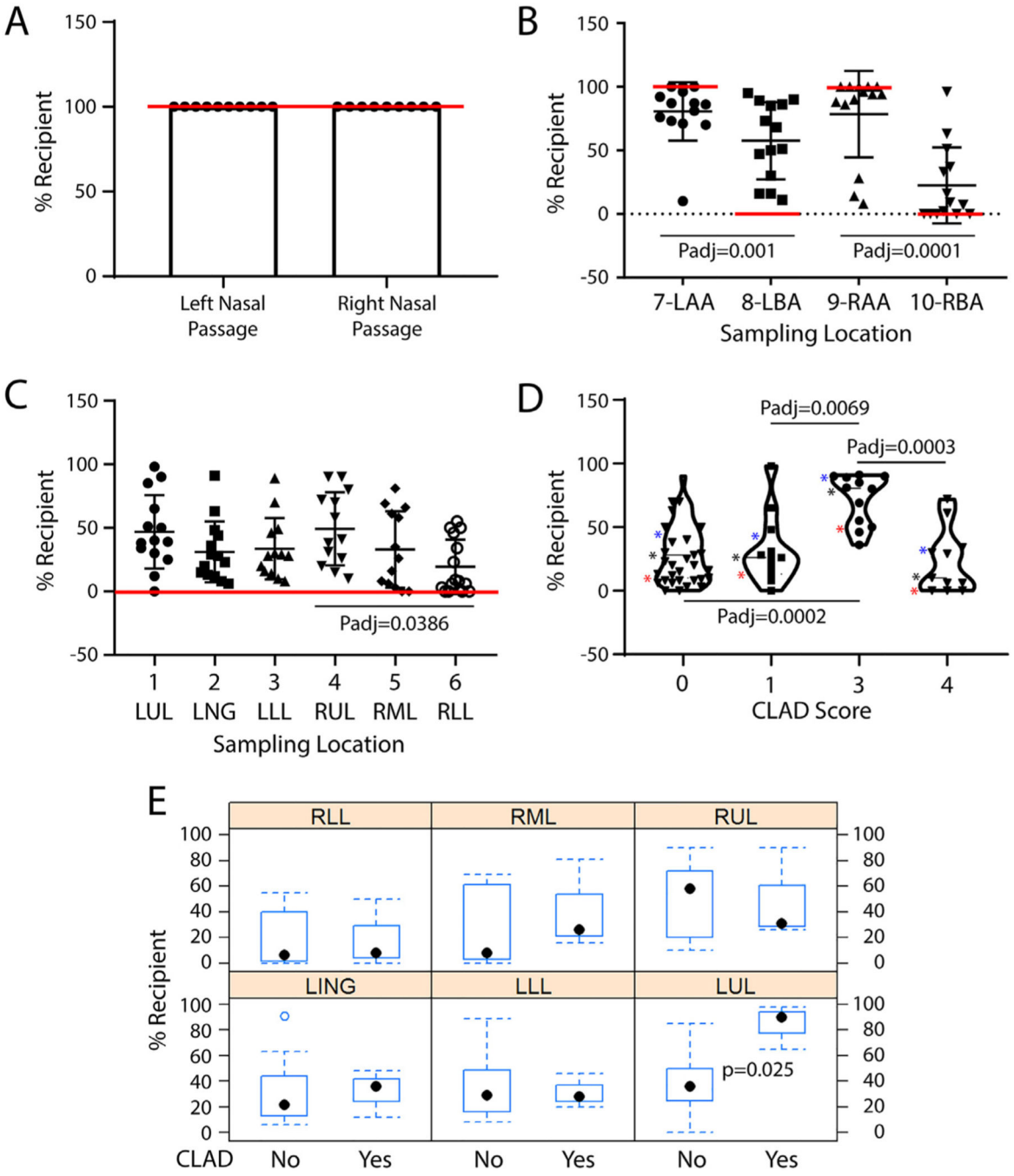

Fig 3.

TSC chimerism in the airways of lung transplant patients. A. TSC chimerism in the nasal respiratory epithelium. B. TSC chimerism at the anastomoses. C. TSC chimerism in the bronchial airways. Values consistent with no chimerism are indicated by the red lines. Symbols represent individual data points. Data are presented as the median with interquartile range, n = 10–13. Differences were evaluated by Kruskal-Wallis test. D. TSC chimerism as a function of CLAD Score. Data are presented as violin plots. Stars: blue-75th percentile, black-median, red-25th percentile. Differences were evaluated by Kruskal-Wallis test. E.

Analysis of differences in TSC chimerism between subjects who had CLAD at the time of sampling and those who were free of CLAD. Box and whisker plots illustrating: range-dotted lines, 25–75 interquartile range-blue rectangle, and median-black dot. Differences were evaluated using a mixed model. (For interpretation of the references to color in this figure legend, the reader is referred to the web version of this article.)

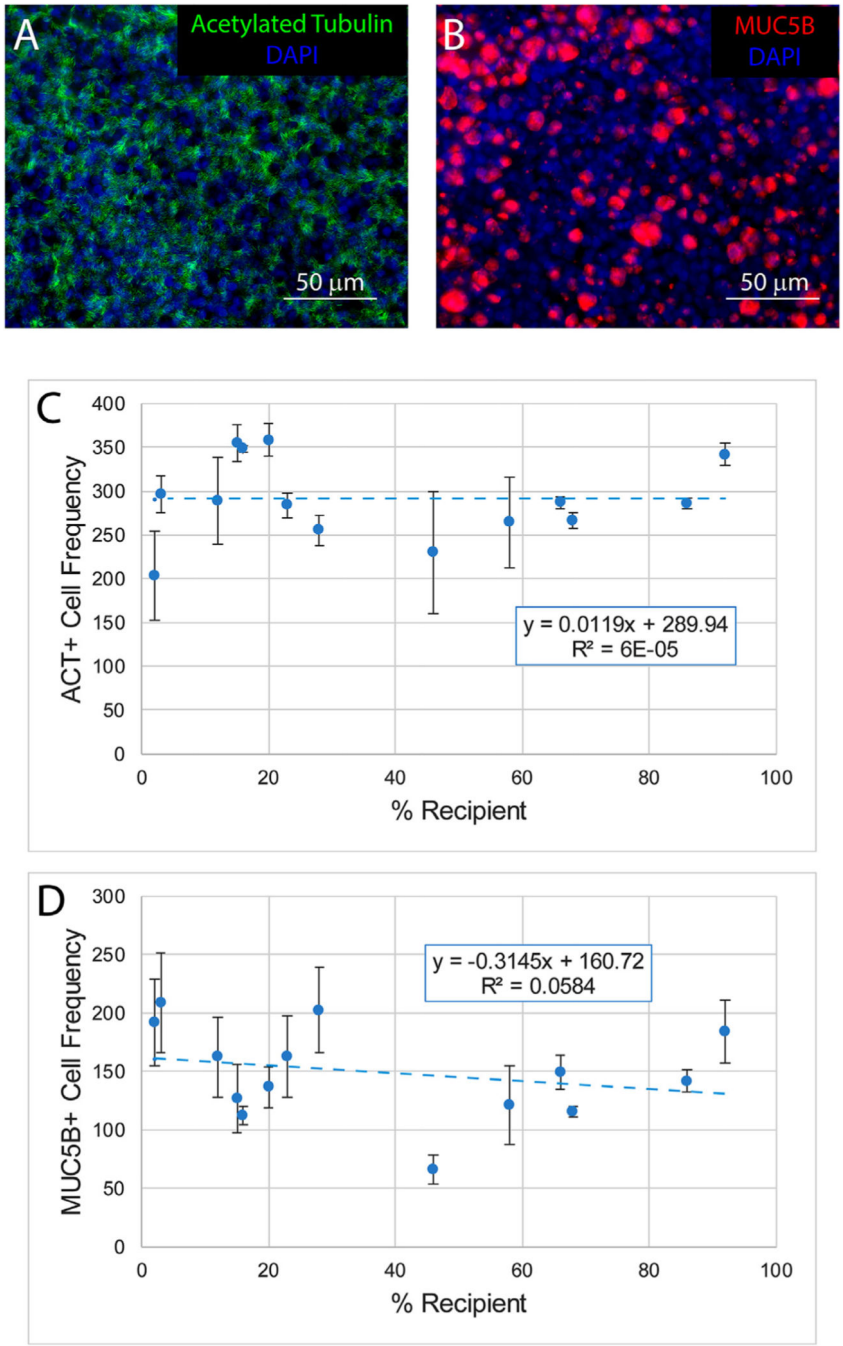

Fig 4.

Impact of TSC chimerism on differentiation. TSC from sampling sites 1–6 were used to generate air-liquid-interface cultures that were differentiated for 21 days in PneumaCult ALI medium. A-B. Representative photomicrographs illustrating ciliated cell differentiation (acetylated tubulin, green) and mucus differentiation (MUC5B, red). Nuclei are stained with DAPI (blue). C. The frequency of ciliated cells as a function of the frequency of recipient TSC. D. The frequency of mucus cells as a function of the frequency of recipient TSC. Data are presented as the mean ± standard deviation, $n = 14$. Blue dashed line: modeling using the

linear regression method. (For interpretation of the references to color in this figure legend, the reader is referred to the web version of this article.)

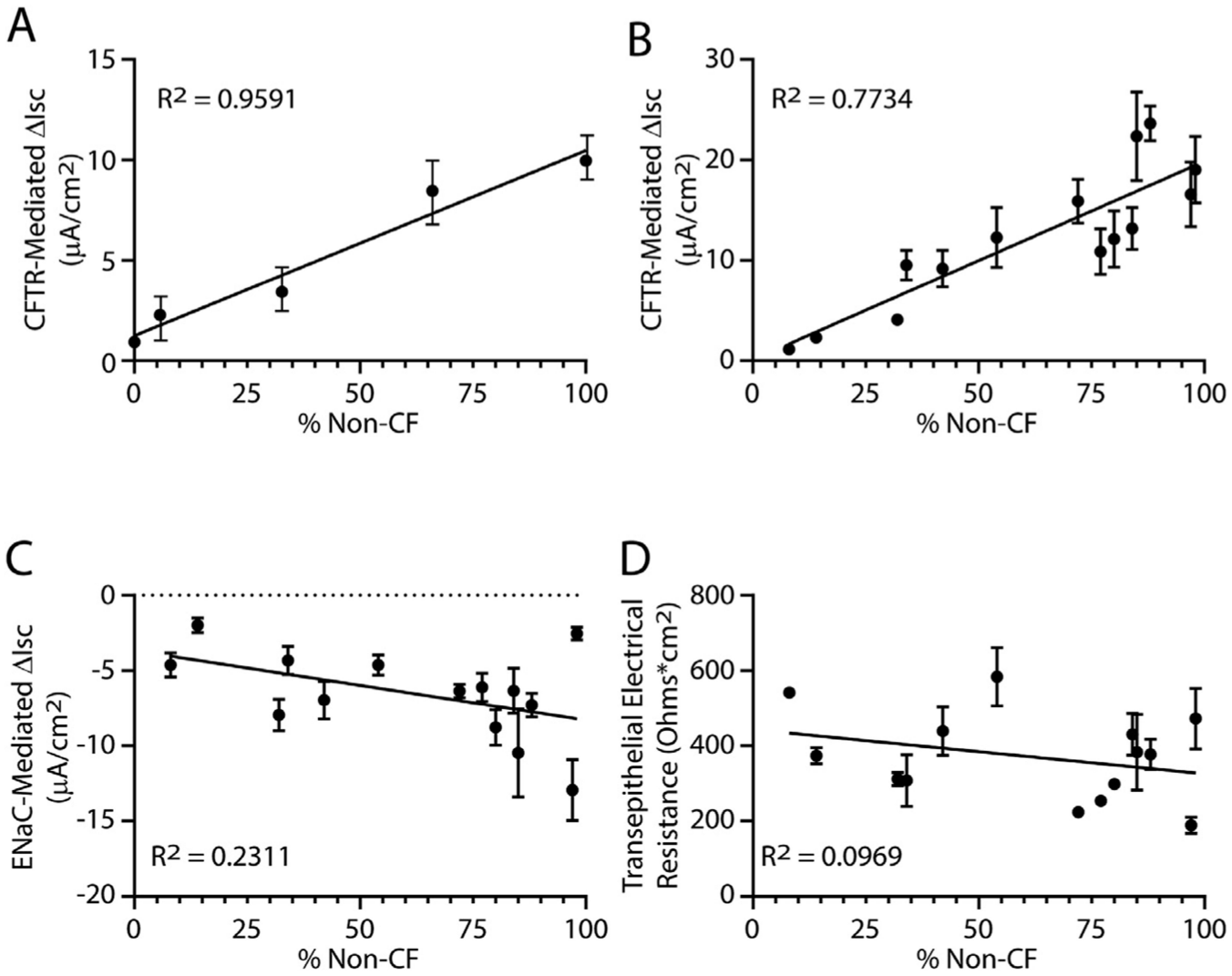

Fig 5.

Impact of TSC chimerism on ion transport. Short circuit currents (ΔIsc) were quantified in well-differentiated day 21 air-liquid-interface (ALI) cultures. A. The change in CFTR dependent short circuit current was quantified in cultures containing a mixture of non-CF and CF TSC. Both forskolin-induced and CFTR inh-172-inhibited currents were measured. The CFTR inh-172 results are presented. The frequency of non-CF cells was determined as indicated in SFigure 1. Data are presented as the mean standard error of the mean (n = 3 technical replicates). B-C. TSC from sampling sites 1–6 were used to generate ALI cultures. On day 21, short circuit currents were assayed. Data are presented as the mean ± standard error of the mean, n = 6 biological replicates. D. CFTR, E. Epithelial sodium channel (ENaC). F. Transepithelial electrical resistance. The black lines in each graph indicate modeling using the linear regression method.